Thermodynamical and stuctural information on photosynthetic systems obtained from electroluminescence kinetics

Marten H. Vos and Hans J. van Gorkom
Department of Biophysics, Huygens Laboratory of the State University, 2300 RA Leiden, The Netherlands

ABSTRACT The relationship between the thermodynamical and structural properties of photosynthetic reaction centers and kinetics and polarization of electric field-induced luminescence was studied. A general model is presented to describe the influence of an electric field on the individual electron transfer rate constants. Comparison of simulations with this model and experimental curves of Photosystem I electroluminescence showed that (*a*) at least three electrogenic electron transfer steps occur: P-700 to A_0(~30%), A_0 to A_1 (~50%), and A_1 to F_A(~20%), (*b*) the midpoint potential of A_1/A_1^- is ~ -0.81 V, and (*c*) the emission moments of the pigments make on average an angle of 67° with the membrane normal. It is concluded that the analysis of electro-luminescence kinetics may be a powerful technique to obtain information on primary processes using relatively intact systems.

INTRODUCTION

The quintessence of photosynthesis is the conversion of the energy of the very short-lived electronically excited state resulting from light absorption by the photosynthetic pigments into the electro-chemical energy of an oxidant and a reductant stable enough to drive biochemical reactions in living cells (1). This energy conversion process takes place in the so-called reaction center, a pigmented protein complex embedded in the photosynthetic membrane, and proceeds via a sequence of electron transfer steps resulting in the transfer of one negative charge across the membrane. Each step is associated, from a thermodynamic point of view, with a loss in standard free energy and, from a structural point of view, with an electron transport vector which can be decomposed into a lateral and a transmembrane, "electrogenic" component. Charge recombination is thus prevented by the physical separation of the charge pair and the combined exothermicity of the electron transfer reactions producing this separation.

By applying an electric potential difference between the opposite sides of the membrane the rate of charge recombination can be influenced and the contributions of the individual electron transfer steps to the stabilization process can be studied. A convenient probe is "electroluminescence," the chlorophyll luminescence resulting from electric field-induced charge recombination. Most of the electroluminescence studies have been performed with blebs (2–4). These are spherical vesicles formed by unfolding of the thylakoid membrane system when chloroplasts are suspended in a hypotonic medium. Presumably due to their large dimensions (diameter ~12 μm [5]) the signal obtained in suspensions of blebs is much larger than that from chloroplasts and can often be measured without averaging. Until 1985 it was thought that all electroluminescence originated from Photosystem II (2–4, 6). Symons and co-workers showed that also Photosystem I electroluminescence can be observed (7, 8).

Since its discovery in 1971 by Arnold and Azzi (6), electroluminescence has been mostly used as a quantitative probe for precursor concentrations (9–11) as a qualitative indicator of electro-genicity (6, 10) and as a probe of the electric and diffusion properties of the membrane (12–14). The temporal and spatial distribution of local fields in the systems used is reflected in the electroluminescence kinetics and polarization and therefore the quantitative interpretation of these properties in terms of electrogenic and thermodynamic parameters is not straightforward and has not been attempted to date. In the present communication we focus on the way the thermodynamic and electrogenic features of the reaction centers are reflected in the electroluminescence kinetics and polarization.

In principle, with knowledge of all parameters involved, the electroluminescence kinetics can be predicted. On the

Dr. Vos's present address is Service de Biophysique, Département de Biologie, Centre d'Etudes Nucleaires Saclay, 91191 Gif-Sur-Yvette Cedex, France.
Address correspondence to Dr. van Gorkom, Department of Biophysics, Huygens Laboratory of the State University, P.O. Box 9504, 2300 RA Leiden, The Netherlands.
Abbreviations used in this paper: DCMU, 3-(3'-4'-dichlorophenyl)-1,1-dimethylurea; E_m, midpoint potential; Mops, morpholinepropanesulphonic acid; PS, Photosystem; TPB, tetraphenylboron, Tris, 2-amino-2-hydroxymethylpropane-1,3-diol.

other hand, insight in unknown parameters may be gained by simulation of kinetics and comparison with experimental data. For this purpose a mathematical model for electroluminescence kinetics and polarization in blebs will be presented. The kinetic model is an extension and a refinement of a model by de Grooth (2). In this earlier model the electroluminescence was considered to arise solely from an alteration of the overall recombination rate with the Boltzmann factor eV/kT. A rough qualitative agreement with the experimental results on PS II was obtained (2). The present model incorporates the membrane potential effect on the rate constants of both the primary and the secondary electron transfer reactions and on triplet formation. Its application to PS I illustrates that this approach reveals information on the electrogenic and thermodynamic properties of the stabilizing reaction.

MATERIALS AND EXPERIMENTAL METHODS

Spinach chloroplasts were prepared and stored as described elsewhere (11). Blebs were formed by diluting a chloroplast suspension with a chlorophyll concentration of 1 mg/ml 200-fold in 1 mM Mops buffer (pH 6.6). The measurements on chloroplasts were performed with samples prepared similarly; only in this case the dilution buffer also contained 0.4 M sucrose. The bleb measurements were performed at least 10 min after dilution. 10 μM DCMU and 5 μM TPB were added for PS I measurements and 10 μM DCMU and 50 μM ferricyanide for PS II measurements (11). In both cases four preflashes spaced at 0.1 s were given before the measuring flash.

The measurements were performed as described in reference 11, except that a curvette with an electrode spacing of 2 mm was used. The emitted light was detected through a Schott RG 665 cut-off filter and a sheet polarizer. For each measurement a fresh sample was taken.

POLARIZATION OF LUMINESCENCE IN BLEBS

The membrane potential generated in a spherical membrane vesicle by an externally applied electric field is proportional to cos θ (see Fig. 1 and Eq. 2 below). When a singlet excited state P* of the primary donor is created by (field-induced) charge recombination the excitation energy equilibrates with the antenna. There is some probability of photon emission before retrapping. The distance of excitation transfer before emission is likely to be very small compared with the bleb size (in the order of magnitude of 1% of the bleb radius), so the emission event can be considered to be localized at the spot of charge recombination. Taking into account the rigid structure of the antenna this implies that the emitted light is polarized, with the polarization depending on the localization on the bleb. The polarization as a function of the angle θ on the bleb (see Fig. 1) can be calculated assuming the

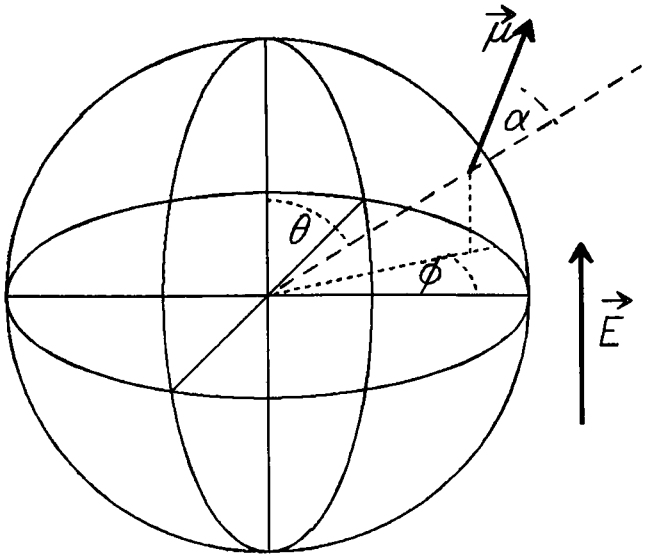

FIGURE 1 Definition of the angles, α, ϕ, and θ describing the orientation of the emission moment $\vec{\mu}$ in the bleb wall. The angle β between the projection of $\vec{\mu}$ on the bleb wall and an axis in the plane of the bleb wall is not shown.

emission moment $\vec{\mu}$ makes a fixed angle α with the membrane normal. Transformtion of $\vec{\mu}$ to the lab frame and integration over ϕ (Fig. 1) and β, the angle of the projection on the membrane with an axis in the plane of the membrane yields for the emission intensities in the directions parallel and perpendicular to the field $I_\parallel$ and $I_\perp$ as a function of θ:

$$I_\parallel(\theta) = I_{tot}\,[-\tfrac{1}{2}\sin^2\theta\,(3\cos^2\alpha - 1) + \cos^2\alpha] \quad (1a)$$

$$I_\perp(\theta) = I_{tot}\,[\tfrac{1}{4}\sin^2\theta\,(3\cos^2\alpha - 1) + \tfrac{1}{2}\sin^2\alpha]. \quad (1b)$$

For the magic angle $\alpha = 54.7°$ no polarization is observed. For all other values the polarization depends on the latitude θ on the bleb. For $\alpha > 54.7°$ the polarization $I_\perp/I_\parallel$ exceeds 1 for $\theta > 54.7°$ (near the poles).

For the actually observed time course of the polarization of the electroluminescence a model for the depletion of the precursor as a function of time and membrane potential is required. If such a model is available the angle α can be derived from the observed polarization. So in principle we have a sensitive method to detect the direction of the emission moment independent of the absorption moment. On the other hand the total amount of emitted light is proportional to $I_\parallel + 2I_\perp$, independent of α. This implies that recombination models can be evaluated independent of an assumption for the value (or the distribution of values) of α, by measuring the electroluminescence in both polarization directions.

A MODEL OF ELECTROLUMINESCENCE IN BLEBS

For the specific case of spherical vesicles a simulation model of electroluminescence kinetics was designed. The features of this model are described in this section.

Membrane potential

The membrane potential V_m as a function of time t after the onset of the pulse and of the external field strength E is (5):

$$V_m(\theta) = 1.5\, R\, E \cos\theta\, [1 - \exp(-t/t_R)] \qquad (2)$$

in which R is the bleb radius, θ the angle between the local radius vector, and $\vec{E}$ and τ is given by

$$t_R = 1.5\, C\rho R \qquad (3)$$

in which C is the specific capacitance of the membrane and ρ the specific resistance of the (internal and external) medium. The product $C\rho$ was determined from external field-induced electrochromic absorbance changes by de Grooth et al. (5) and was found to be 2 s/m in their preparations. A similar value was expected in our preparations.

At membrane potentials higher than ~1 V dielectric breakdown occurs (2, 15, 16). This implies that the membrane is perforated, its conductivity is drastically increased, and its membrane potential decreased. The mechanism is not fully understood and no well-established formalism is available to describe the effects of this phenomenon on the membrane potential. It was recently shown that a phenomenological description, in which the enhancement of the conductivity is proportional to the applied membrane potential in excess of a threshold, is adequate (16). Here we avoid the problem by considering only membrane potentials well below 1 V.

Recombination kinetics

In earlier models (2, 17) it was assumed that the field enhancement of the back reaction rate was equal to the Boltzmann factor $\exp(eV/kT)$, in which e the electron charge, V the induced potential over the donor–acceptor pair, k the Boltzmann constant, and T the absolute temperature. Here we present a more refined model, which takes into account different pathways of recombination and field-induced alteration of dynamical rate constants in those pathways.

Consider a photosystem which consists of a donor P and a chain of acceptors $A_0 \ldots A_n$ embedded in an antenna of Chl molecules and (nonphysiological) conditions in which $P^+A_n^-$ is formed as a "stable" charge pair. We will assume that charge recombination occurs only via thermally activated processes, with $P^+A_0^-$ as the intermediate state, resulting in either the singlet (Chl*) or the triplet (P^T) excited state (see Fig. 2). The differences in standard free energy ΔG_i^0 (between the states $P^+A_i^-$ and $P^+A_{i-1}^-$) and ΔG_*^0 (between the states P* and $^1[P^+A_0^-]$) and ΔG_T^0 (between the states P^T and $^3[P^+A_0^-]$) are altered by a term $d_i eV_m$ in the presence of a membrane potential V_m. Here d_i indicates the dielectrically weighted transmembrane distance between A_{i-1} and A_i ($\Sigma d_i = 1$, $i = 0$ represents the primary charge separation). V_m is defined as positive when it enhances the back reaction:

$$\Delta G_i^0(V_m) = \Delta G_i^0(0) + d_i eV_m. \qquad (4)$$

The influence of the field on the rate constants k_i (forward reactions, see Fig. 2) and k_{-i} (backward reactions) is evaluated with the thermodynamical rate theory of Marcus (18). According to this theory

$$k_i = k_{0i} \exp[-\lambda_i(1 + \Delta G_i^0/\lambda_i)^2/4kT] \qquad (5a)$$

$$k_{-i} = k_{0i} \exp[-\lambda_i(1 - \Delta G_i^0/\lambda_i)^2\, 4kT] \qquad (5b)$$

with k_{0i} an intrinsic rate constant, ΔG_i^0 chosen negative, and λ_i the reorganizational energy (positive, see Fig. 3).

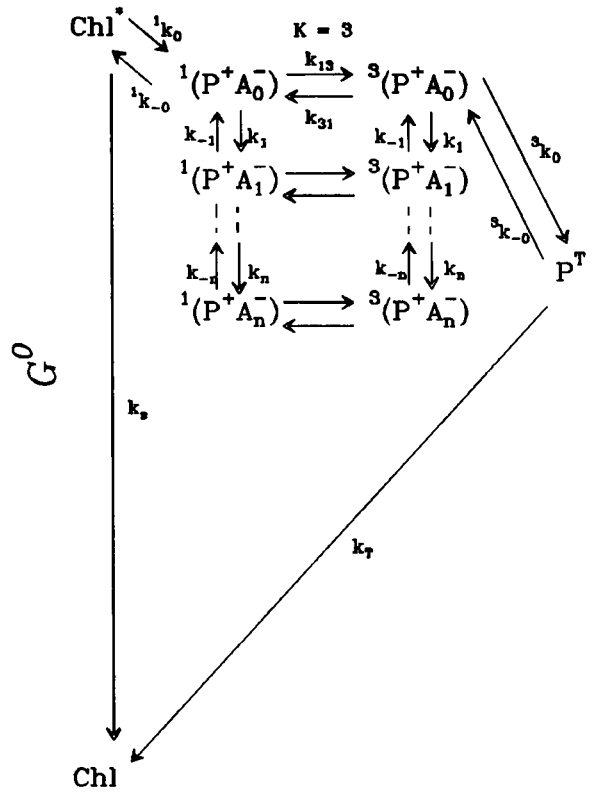

FIGURE 2 Model for electron transport in the reaction center. Spin dephasing reactions were described by an equilibrium constant K (see text) and direct recombination to the ground state was neglected.

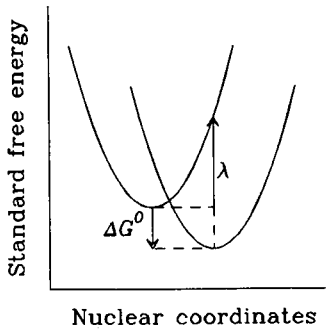

FIGURE 3 Definition of the standard free energy difference ΔG^0 and the reorganizational energy λ for an electron transport reaction. The x-axis represents a multidimensional system.

Using Eq. 4 we obtain for the rate constants:

$$k_i(V_m) = k_i(0) \cdot \exp\{-d_i e V_m [d_i e V_m/\lambda_i + 2 + 2\Delta G_i^0(0)/\lambda_i]/4kT\} \quad (6a)$$

$$k_{-i}(V_m) = k_{-i}(0) \cdot \exp\{-d_i e V_m [d_i e V_m/\lambda_i - 2 + 2\Delta G_i^0(0)/\lambda_i]/4kT\}. \quad (6b)$$

So, when all zero-field rate constants $k_i(0)$ and $k_{-i}(0)$, reorganizational energies λ_i and weighted dielectric distances d_i are known the field-induced rate constants can be calculated. For activationless processes $\lambda_i = -\Delta G_i^0$. In this case the expressions for the rate constants simplify to:

$$k_i(V_m) = k_i(0) \exp\{(d_i e V_m)^2/(4\Delta G_i^0(0)\, kT]\} \quad (7a)$$

$$k_{-i}(V_m) = k_{-i}(0) \cdot \exp\{d_i e V_m [d_i e V_m/\Delta G_i^0(0) + 4]/4kT\}. \quad (7b)$$

The model presented here only accounts for secondary reactions at the acceptor side. Secondary reactions at the donor side may be treated analogously. Stabilizing forward reactions beyond the precursor state $P^+A_n^-$ may also be incorporated.

When P* is formed by charge recombination it will equilibrate with the antenna molecules Chl with an equilibrium constant K^*. For the calculation of the rates $^1k_{-0}$ and $^1k_0$ (see Fig. 2) in the presence of an electric field first the rates $^1k_{-0}$ and k_{cs} are calculated, in which k_{cs} is the rate of charge separation from P*. Here Eq. 7 is used and ΔG_i^0 is obtained from the free energy levels of P* and $^1(P^+A_0^-)$. Then the equilibration with the antenna is taken into account by calculating $^1k_0$ using $^1k_0 = k_{cs}/K^*$.

Electroluminescence kinetics

Using these ingredients the electroluminescence kinetics are now computed as follows. A point at latitude θ on a bleb with radius R is considered. The whole system is described by a set of coupled linear differential equations describing the time course of the population of the different redox states. At the onset of the pulse, $t = 0$, all centers are taken to be in the state $P^+A_n^-$, of which 25% are in $^1(P^+A_n^-)$ and 75% in $^3(P^+A_n^-)$. The new population of all states for $t = \delta t$ with $\delta t \ll \tau$, the risetime of the membrane potential, is now calculated by solving the set of linear equations and inserting the initial conditions. For $t = \delta t$ the new value for the membrane potential is calculated according to Eqs. 2 and 3. From this value new rate constants are calculated using Eqs. 7 and the whole sequence is repeated. The induced luminescence is taken to be proportional to the concentration of P* and calculated in the two polarization directions using Eqs. 1. The total emission at each time is obtained by integration over the latitude θ and the bleb size distribution.

It should be mentioned that the model of Fig. 2 does not correctly describe the spin dephasing reactions because solutions of the stochastic Liouville equation should be used (19) rather than linear differential equations. However, the time scale of the recombination reactions described by our model, microseconds, is much longer than the time scale of spin dephasing, which is in the order of 10–100 ns (19) and hence the spins can be considered as equilibrated and described as in Fig. 2. It was checked that the results were independent of the choice of the value for the rate constants for spin dephasing within the above range (see section below).

SIMULATIONS OF PHOTOSYSTEM I ELECTROLUMINESCENCE

Kinetics

The kinetics of the population of the singlet excited state of chlorophyll in the PS I antenna, Chl*, induced by an external electric field pulse were simulated for the case that the reaction centers are in the state $P\text{-}700^+F_A^-$ at the onset of the pulse. The distribution of bleb sizes was determined by phase contrast microscopy as before (5). The distribution is shown in Fig. 4 (*inset*) and was similar to that of de Grooth et al. (5), but shifted slightly toward larger bleb sizes. This is possibly due to the use of chloroplasts prepared from laboratory grown spinach leaves instead of leaves from local shops. Simulations were made for external field strengths of 500 and 650 V/cm and compared with experimental curves. The latter were obtained with a delay of 50 ms between the flash and the pulse to avoid contributions from the state $P\text{-}700^+F_B^-$ (11). We will use half-times τ in the following discussion with the same indexing as the corresponding rate constants k.

We first tried the model of Fig. 2 with $n = 1$; i.e., in the

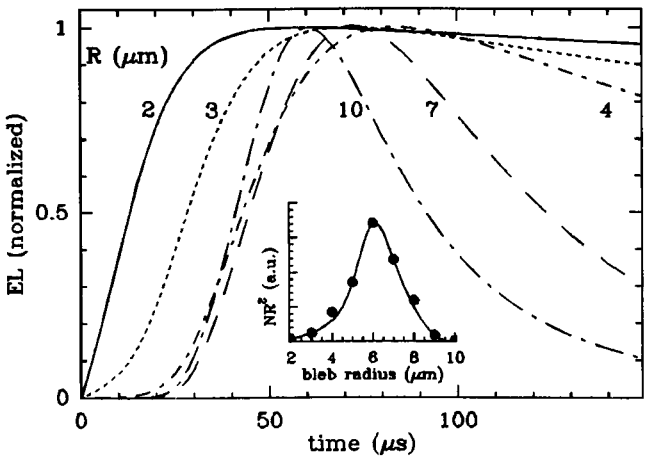

FIGURE 4 Simulated electroluminescence for blebs with different radii. The parameters used for the simulations are listed in Table 1 (*bold values*). (*Inset*) Area-weighted bleb size distribution.

TABLE 1 Kinetic simulation parameters

E_m(P-700$^+$/P-700)	**+0.48** *V*	K^*	**30** (*20 . . . 200*)
E_m(P-700*/P-700$^+$)	**−1.29** *V*		
E_m(P-700^T/P-700$^+$)	**−0.79** *V*		
E_m(A_0/A_0^-)	**−1.01** *V*		
E_m(A_1/A_1^-)	**−0.81** (*−0.83 . . . −0.79*) *V*		
E_m(F_A/F_A^-)	**−0.55** *V*		
τ_s	**2.0** (*0.5 . . . 10.0*) *ns*	d_1	**0.50** (*0.40 . . . 0.60*)
τ_T	**6** *μs*	d_2	**0.175** (*0.15 . . . 0.20*)
τ_{cs}*	**3** (*1 . . . 15*) *ps*	$C\rho$	**2.5** (*2.0 . . . 3.0*) *s/m*
$^3\tau_0$	**0.01** (*0.01 . . . 100*) *ns*		
τ_1	**20** *ps*		
τ_2	**200** *ns*		
τ_{13}	**10** (*1 . . . 100*) *ns*		
τ_R‡	∞ (*0.1 . . . ∞*) *μs*		

Half-times τ, midpoint potentials, and other parameters used in the simulations. The bold values indicate the values used for the curves in Fig. 4; indicate the range of variation of the parameters as described in the text.

Half-time of the primary charge separation from P-700 to ^{1}(P-700$^+$ A_0^-).

‡Direct recombination from ^{1}(P-700$^+$ A_0^-); not displayed in Fig. 2 (see text).

model F_A = A_1 and recombination from P-700$^+F_A^-$ proceeds via the state P-700$^+A_0^-$ only. Using known values for the kinetic rates and midpoint potentials (see below) the simulated curves displayed much faster kinetics than the experimental curves. If it was assumed that $E_m(A_0/A_0^-) = -1.01$ V (11) the simulated curves would only reasonably fit with the experimental curves if τ_1, the half-time of A_0^- reoxidation by forward electron transport, was chosen in the nanosecond time range. However, this would imply that the half-time of back reaction from F_A^- to A_0^- is more than 70 ms, the charge recombination time of P-700$^+F_A^-$ (11). Consequently the model with $n = 1$ is too simple and a slower electron transport step must be taken into account. We thus proceeded with the model as in Fig. 2 with $n = 2$. The PS I electron acceptors A_1 and F_A are now represented by "A_1" and "A_2" in Fig. 2.

The half-times and standard free energies used in the model are listed in Table 1. The literature provided values for E_m(P-700$^+$/P-700) (+0.48 V [20]), $E_m(F_A/F_A^-)$ (−0.55 V [20]), τ_T (6 μs [21]), τ_1 (20 ps [22]), and τ_2 (200 ns [23, 24]). For $E_m(A_0/A_0^-)$ a value of −1.01 V was used (11). It has been shown that in bacterial reaction centers the entropy contributions to the singlet and triplet excited states are negligible (25, 26). Assuming that this is also the case in PS I, E_m(P-700$^+$/P-700), the energy of photons of 700 and 980 nm (the phosphorescence wavelength of chlorophyll *a* [27]) yield E_m(P-700*/P-700$^+$) and E_m(P-700^T/P-700$^+$). They were calculated to be −1.29 and −0.79 V, respectively. The same value for E_m(P-700^T/P-700$^+$) can be calculated from $E_m(F_A/F_A^-)$ and the decay half-times of the states P-700$^+F_A^-$ in the absence of an electric field (70 ms [11]) and of P-700^T (6 μs, see above). Taking into account that ~200 chlorophylls per PS I reaction center are present and that their Q_Y transitions are at ~20 nm shorter wavelength than that of P-700 we estimated K^* to be 30. The forward electron transport reactions were assumed to be activationless (28–30). At first the other rate constants were chosen as in Table 1. $E_m(A_1/A_1^-)$, the parameters d_1 and d_2, describing the transmembrane distance from A_0 to A_1 and from A_1 to F_A, respectively, relative to the total membrane thickness (it was assumed that the P-700$^+F_A^-$ charge pair spans the whole membrane, i.e., $d_0 = 1 - d_1 - d_2$) and the electric constant $C\rho$ were varied.

Fig. 4 shows the dependence of the electroluminescence on the bleb size. For small blebs ($R < 4$ μm) the radius determines the rise kinetics (Eq. 3) and the decay is relatively slow due to the slow exhaustion of the precursors. For larger blebs the precursors are exhausted during the rise of the field already and this limits the rise time of the signal. The decay of the signal becomes more polyphasic with larger bleb radius within the time range displayed. The amplitude of the signal depends strongly on the bleb size, due to the membrane potential dependence both of the recombination kinetics and of the luminescence yield. Hence the overall electroluminescence kinetics observed are largely determined by the larger blebs.

In Fig. 5 simulations with the measured distribution of bleb sizes are displayed. $E_m(A_1/A_1^-)$, d_1, d_2, and $C\rho$ are varied and it can be seen that the simulated curves are very sensitive to changes in these parameters. Expectedly, $C\rho$ strongly influences the lag phase of the signal. d_1

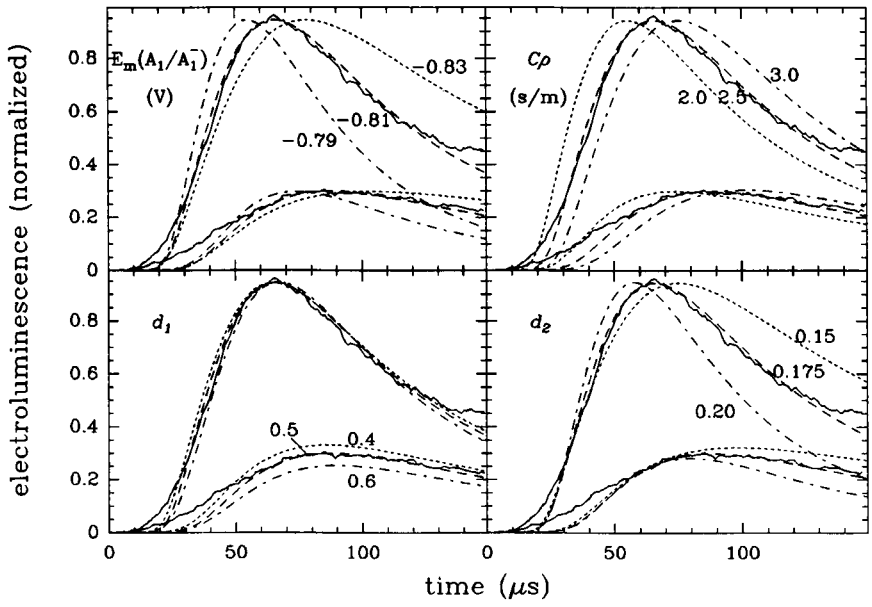

FIGURE 5 Simulated (*dashed*) and measured (*solid*) curves of PS I electroluminescence, $EL_\parallel$ and $EL_\perp$ were measured during a pulse given 50 ms after the last of five flashes; $EL_\parallel + 2\ EL_\perp$ is displayed (average of 20 traces). The parameters used for the simulations are listed in Table 1 (*bold values*); in each panel one of the parameters E_m A_1/A_1^-, $C\rho$, d_1, and d_2 is varied as indicated. (*Upper curves in each panel*) 650 V/cm; (*lower curves*) 500 V/cm. The curves are normalized at the peak amplitude of the 650 V/cm curves.

merely determines the relative peak amplitude of the curves at the different external field strengths. $E_m(A_1/A_1^-)$ and d_2 mainly influence the decay of the signal during the pulse. The simulated curves fit best to the experimental curves for $E_m(A_1/A_1^-) = -0.81$ V, $d_1 = 0.5$, $d_2 = 0.175$, and $C\rho = 2.5$ s/m. The value of 2.5 s/m that we found for $C\rho$ is close to the value of 2.0 s/m reported by de Grooth et al. (5) in similar preparations, and significantly larger than reported in references 31 and 32. The origin of this discrepancy is not clear.

Variation of most of the other parameters within the ranges listed in Table 1 did not yield significantly different normalized simulated curves. With regard of the parameters k_{13} (and k_{31}) this justifies the use of the simplified description of spin dephasing (see above). The curves were found to be virtually independent of the values of $^1k_0$ and $^3k_0$. This indicates that the rates of changes in the eqilibrium concentrations Chl*/^{1}(P-700$^+$A$_0^-$) and P-700^T/^{3}(P-700$^+$A$_0^-$) are not rate limiting for the electroluminescence kinetics. Variation is k_s, K^*, and k_1 all lead to changes in the relative peak amplitudes of the curves at different field strengths similar to that of d_1. This reflects the influence of the field on the competition between decay to the ground state via Chl* and reformation of ^{1}(P-700$^+$A$_1^-$) once (P-700$^+$A$_0^-$) has been formed. The largest uncertainty arises from k_s; if $\tau_s = 1$ ns a value of 0.6 for d_1 is needed to fit the experimental data.

It was checked that a possible direct and field-insensitive recombination to the ground the state ^{1}(P-700$^+$A$_0^-$) with a half-time of 10 ns gave virtually the same results as when such a decay path was omitted (see also reference 11).

It should be noted that the model with three electron transport steps that we used still is a minimal model. F_X may act as a redox intermediate between A_1 and F_A (20). If this is the case the model with $n = 3$ may be too simple; however in view of the relatively low electrogenicity of the electron transport between A_1 and F_A deviations from a model with $n = 4$ are expected to be small. Indeed, calculations with a model in which F_X was taken into account as an intermediate acceptor ($E_m[F_X/F_X^-] = -0.705$ V [20]; electron transport from F_X^- to F_A^- was assumed to take 2 μs or less) the simulations did not deviate much from the best fitting curves in Fig. 5 if it was assumed that A_1F_X spans more than 30% of the dielectric distance between A_1 and F_A (not shown). This seems a reasonable assumption and hence we conclude that the model with 3 electron transfer steps is sufficient to describe the PS I electroluminescence kinetics.

The omission of F_X in our model could not explain the deviations of the experimental curves and the best fitting simulated curves during the lag phase and in the decay phase (>140 μs). Another explanation for this discrepancy may be that we did not take the patches on the bleb wall into account in our simulations; also the relative

amount of small blebs may be underestimated. Patches and small blebs are expected to give rise to a faster rising and slower decaying signal than larger blebs (Fig. 4). However, the amplitude of the electroluminescence arising from those blebs is expected to be much lower than that from larger blebs and to explain the observed kinetics it must be assumed that the amount of material in the larger blebs is orders of magnitude smaller than that in the smaller blebs. This is not realistic. Hence the deviation of the simulated and experimental curves during the lag phase remains to be clarified. On the other hand, a small underestimation of the amount of large blebs, which strongly influence the overall signal, may explain the deviation at longer times, by their more polyphasic kinetics.

Our results indicate that the primary charge separation P-700A_0 → P-700$^+A_0^-$ spans ~30% of the membrane, electron transport from A_0^- to A_1^- ~50% and the reduction of F_A by A_1^- ~20%. This is consistent with the qualitative result of an earlier study on PS I electroluminescence (11) that both the primary change separation and subsequent electron transport is electrogenic. Trissl et al. (33) reported that electrogenic electron transport occurs within 50 ps and that no electrogenic steps occur in the time range of 50 ps to 50 ns. Our results are consistent with these findings and further demonstrate the presence of an electrogenic step which occurs on a longer time scale.

The value of −0.81 V for $E_m(A_1/A_1^-)$ which we find has interesting implications for physiological forward electron transport in the absence of an external field. With $E_m(A_0/A_0^-) = -1.01$ V and $\tau_1 = 20$ ps we find $\tau_{-1} = 60$ ns. Hence backward electron transport from A_1^- to A_0 is faster than forward transport to F_A and, as spin dephasing also takes place in the nanosecond time range, the state ^{3}(P-700$^+A_0^-$) is populated in equilibrium with ^{3}(P-700$^+A_1^-$). From here the state P-700$^+$ may be populated depending on the rate of triplet recombination $^3k_0$. If this reaction takes ~700 ps, the upper limit for $^3\tau_0$ deduced for this reaction in reference 11, the net reaction from ^{3}(P-700$^+A_1^-$) to P-700^T takes ~2 μs, which is 10 times slower than τ_2 (200 ns). Centers where P-700^T has been formed will have a high chance to decay to the ground state ^{1}P-700 as the half-time of charge separation from P-700^T in this case is ~5 μs, similar to τ_T (6 μs). If triplet recombination occurs much faster than 700 ps P-700^T may be formed in equilibrium with ^{3}(P-700$^+A_1^-$), which has a similar midpoint potential. In this case the loss from P-700^T is much less, however, because the rate of charge separation from P-700^T, $^3k_{-0}$, is much higher. In both cases the loss by the pathway via P-700^T amounts to a few percent.

Polarization

Fig. 6 shows the simulations of the polarization of the electroluminescence using the parameters which gave the best fit of the total electroluminecence kinetices. Also, the measured curves are shown. The simulated and experimental curves both display an initial rise which is followed by a decay; the maximum is reached before the total electroluminescence reaches its maximal value (cf. Fig. 5). The initial rise reflects the increasing population of the P-700* state of reaction centers around $\theta = 0°$ (the pole facing the negative electrode) in the bleb wall. The following decay reflects the exhaustion of the precursors at increasing distance from the pole. A similar initial rise was observed in the polarization of the PS II electroluminescence (not shown); this rise has not been noted in earlier work (2), presumably due to a too low signal-to-noise ratio.

It can be seen that the amplitude of the curve is very sensitive to the angle α between the emission moment and the membrane normal. Comparison of the simulation with the experimental curves indicate that α is ~67°. Our data are not spectrally resolved and hence this value represents an average over the emission spectrum, which

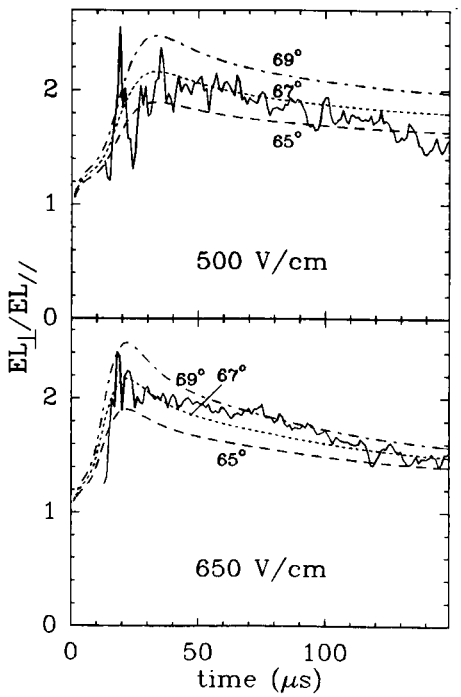

FIGURE 6 Simulated (*dashed*) and measured (*solid*) polarization ($EL_\perp/EL_{//}$) curves of PS I electroluminescence. The experimental curves are obtained from the same data as those in Fig. 5. The parameters used for the simulations are listed in Table 1 (*bold values*). The angle α between the membrane normal and the emission moment is varied as indicated.

peaks at ~690 nm and has a broad shoulder on the red side (not shown, see reference 8). Nevertheless our result may be compared with the angles of 59° to 65° for the absorption dipoles of the Photosystem I antenna pigments, deduced by Kramer and Amesz (34) from fluorescence detected linear dichroism at low temperature. Our result is in qualitative agreement with these data, if one takes into account that the latter were calculated on the assumption that magnetic orientation of chloroplasts gives perfect alignment of the chloroplast lamellae.

CONCLUDING REMARKS

We have shown that analysis of electroluminescence traces may yield quantitative information on the thermodynamics and electrogenicity of electron transport in the reaction center. To analyze the electroluminescence kinetics quantitatively the experimental data have to be compared with model calculations. This was done for PS I. The calculated kinetics showed to be very sensitive to the electrogenicity of the electron transfer steps and the midpoint potential of A_1/A_1^-. It was shown that at least three electrogenic electron transfer steps are electrogenic and that $E_m(A_1/A_1^-)$ is ~ -810 mV. Both the experimental and the theoretical electroluminescence polarization curves displayed a maximum; this phenomenon was hitherto unknown. It is concluded that electroluminescence, easily measured with conventional techniques on relatively intact systems, can provide detailed quantitative structural and functional information on the primary processes of photosynthesis. Similar strategies as applied in this paper for PS I may be used to obtain quantitative information on PS II and reaction centers of photosynthetic bacteria.

We thank M. L. van der Erf, A. H. M. de Wit and M.C. Nieveen for technical assistance and Drs. J. Amesz and A. J. Hoff for reading the manuscript.

This research was supported by the Netherlands Foundation for Chemical Research (SON), financed by the Netherlands Organization for Scientific Research (NWO).

Received for publication 27 March 1990 and in final form 4 June 1990.

REFERENCES

1. van Gorkom, H. J. 1986. Photochemistry of photosynthetic reaction centres. *Bioelectrochem. Bioeng.* 16:77–87.
2. de Grooth, B. G., and H. J. van Gorkom. 1981. External electric field effects on prompt and delayed fluorescence in chloroplasts. *Biochim. Biophys. Acta.* 635:445–456.
3. Ellenson, J. L., and K. Sauer. 1976. The electrophotoluminescence of chloroplasts. *Photochem. Photobiol.* 23:113–123.
4. Farkas, D. L., R. Korenstein, and S. Malkin. 1980. Electroselection in the photosynthetic membrane: polarizedluminescence induced by an external electric field. *FEBS (Fed. Eur. Biochem. Soc.) Lett.* 120:236–242.
5. de Grooth, B. G., H. J. van Gorkom, and R. F. Meiburg. 1980. Electrochromic absorbance changes in spinach cholorplasts induced by an external field. *Biochim. Biophys. Acta.* 589:299–314.
6. Arnold, W. A., and R. Azzi. 1971. The mechanism of delayed light production by photosynthetic organisms and a new effect of electric fields on chloroplasts. *Photochem. Photobiol.* 14:233–240.
7. Symons, M., R. Korenstein, and S. Malkin. 1985. External electric-field effects on photosynthetic vesicles. The relationship of rapid and slow phases of electrophotoluminescence in hypotonically swollen chloroplasts to PS I and PS II activity. *Biochim. Biophys. Acta.* 806:305–310.
8. Symons, M., S. Malkin, and D. L. Farkas. 1987. Electric-field-induced luminescence emission spectra of Photosystem I and Photosystem II from chloroplasts. *Biochim. Biophys. Acta.* 894: 578–582.
9. Babcock, G. T., C. T. Yerkes, and W. J. Buttner. 1981. Static and dynamic electrostatic phenomena in chloroplast Photosystem II. *In* Photosynthesis. G. Akoyunoglou, editor. Balaban International Science Services, Philadelphia, PA. I:637–645.
10. van Gorkom, H. J., R. F. Meiburg, and L. J. de Vos. 1986. Thermodynamics of the charge recombination in photosystem II. *Photosynth. Res.* 9:55–62.
11. Vos, M. H., and H. J. van Gorkom. 1988. Thermodynamics of electron transport in Photosystem I studied by electric field-stimulated charge recombination. *Biochim. Biophys. Acta.* 934: 293–302.
12. Farkas, D. L., R. Korenstein, and S. Malkin. 1984. Electrophotoluminescence and the electrical properties of the photosynthetic membrane. I. Initial kinetics and the charging capacitance of the membrane. *Biophys. J.* 45:363–373.
13. Farkas, D. L., S. Malkin, and R. Korenstein. 1984. Electrophotoluminescence and the electrical properties of the photosynthetic membrane. II. Electric field-induced electrical breakdown of the photosynthetic membrane and its recovery. *Biochim. Biophys. Acta.* 767:507–514.
14. Brumfeld, V., I. R. Miller, and R. Korenstein. 1989. Electric-field induced lateral mobility of photosystem I in the photosynthetic membrane. A study of electrophotoluminescence. *Biophys. J.* 56:607–614.
15. Zimmermann, U., G. Pilwat, F. Beckers, and F. Riemann. 1976. Effects of external electrical fields on cell membranes. *Bioelectrochem. Bioenerg.* 3:58–83.
16. Kinosita, K., I. Ashikawa, N. Saita, H. Yoshimura, H. Itoh, K. Nagayama, and A. Ikegami. 1988. Electroporation of cell membrane visualized under a pulsed-laser fluorescence microscope. *Biophys. J.* 53:1015–1019.
17. Meiburg, R. F. 1985. Orientation of components and vectorial properties of photosynthetic reaction centers. Ph.D. thesis. University of Leiden, The Netherlands. 105 pp.
18. Marcus, R. A., and N. Sutin. 1985. Electron transfers in chemistry and biology. *Biochim. Biophys. Acta.* 811:265–322.
19. Hoff, A. J. 1981. Magnetic field effects on photosynthetic reactions. *Q. Rev. Biophys.* 14:599–665.
20. Rutherford, A. W., and P. Heathcote. 1985. Primary photochemistry in photosystem-I. *Photosynth. Res.* 6:295–316.

21. Sétif, P., G. Hervo, and P. Mathis. 1981. Flash-induced absorption changes in Photosystem I. Radical pair or triplet state formation? *Biochim. Biophys. Acta.* 638:257–267.

22. Shuvalov, V. A., A. M. Nuijs, H. J. van Gorkom, H. W. J. Smit, and L. N. M. Duysens. 1986. Picosecond absorbance changes upon selective excitation of the primary donor P-700 in Photosystem I. *Biochim. Biophys. Acta.* 850:319–323.

23. Brettel, K. 1988. Electron transfer from A_1^- to an iron-sulfer center with $t_{1/2}$ = 200 ns at room temperature in Photosystem I. Characterization by flash absorption spectroscopy. *FEBS (Fed. Eur. Biochem. Soc.) Lett.* 239:93–98.

24. Bock, C. H., A. J. van der Elst, K. Brettel, and D. Stehlik. 1989. Nanosecond electron transfer kinetics in photosystem I as obtained from transient EPR at room temperature. *FEBS (Fed. Eur. Biochem. Soc.) Lett.* 247:91–96.

25. Ogrodnik, A. M. Volk, R. Letterer, R. Feick and M. E. Michel-Beyerle. 1988. Determination of free energies in reaction centers of *Rb. sphaeroides*. *Biochim. Biophys. Acta.* 936:361–371.

26. Goldstein, R. A., L. Takiff, and S. G. Boxer. 1988. Energetics of initial charge separation in bacterial photosynthesis: the triplet decay rate in very high magnetic fields. *Biochim. Biophys. Acta.* 934:253–263.

27. Krasnovskii Jr., A. A. 1982. Delayed fluorescence and phosphoresence of plant pigments. *Photochem. Photobiol.* 36:733–741.

28. Parson, W. W., and B. Ke. 1982. Primary photochemical reactions. *In* Photosynthesis. Govindjee, editor. Academic Press, New York. 331–385.

29. Creighton, S., J.-K. Hwang, A. Warshel, W. W. Parson, and J. Norris. 1988. Simulating the dynamics of the primary charge separation process in bacterial photosynthesis. *Biochemistry.* 27:774–781.

30. Krishtalik, L. I. 1989. Activationless electron transfer in the reaction centre of photosynthesis. *Biochim. Biophys. Acta.* 977: 200–206.

31. Farkas, D. L., R. Korenstein, and S. Malkin. 1984. Electrophotoluminescence and the electrical properties of the photosynthetic membrane. *Biophys. J.* 45:363–373.

32. Arnold, W. M., B. Wendt, U. Zimmerman, and R. Korenstein. 1985. Rotation of a swollen thylakoid vesicle in a rotating electric field. Electrical properties of the photosynthetic membrane and their modification by ionophores, lipophylic ions, and pH. *Biochim. Biophys. Acta.* 813:117–131.

33. Trissl, H.-W., W. Leibl, J. Deprez, A. Dobek, and J. Breton. 1987. Trapping and annihilation in the antenna system of Photosystem I. *Biochim. Biophys. Acta.* 893:320–332.

34. Kramer, H. J. M., and J. Amesz. 1982. Anisotropy of the emission and absorption bands of spinach chloroplasts measured by fluorescence polarization and polarized excitation spectra at low temperature. *Biochim. Biophys. Acta.* 682:201–207.